Chemical Physics Letters 595–596 (2014) 256–259

Contents lists available at ScienceDirect

Chemical Physics Letters

journal homepage: www.elsevier.com/locate/cplett

The high-resolution infrared spectrum of the $\nu_3 + \nu_8$ combination band of jet-cooled propyne

Dongfeng Zhao *, Harold Linnartz

Sackler Laboratory for Astrophysics, Leiden Observatory, University of Leiden, PO Box 9513, NL 2300 RA Leiden, The Netherlands

ARTICLE INFO

Article history:
Received 28 January 2014
In final form 7 February 2014
Available online 15 February 2014

ABSTRACT

The high-resolution infrared spectrum of the $\nu_3 + \nu_8$ combination band of propyne (CH_3—C≡CH) is presented for the first time. Continuous-wave cavity ring-down spectroscopy is used to measure this weak infrared band in the 3175 cm^{-1} region using a supersonic free jet. The rotational analysis of the experimental spectrum results in accurate spectroscopic parameters for the $\nu_3 + \nu_8$ combination vibrational state. Severe perturbations are found for $K = 3$ and 4 rotational levels that are likely due to near-resonant or non-resonant interactions between the $\nu_3 + \nu_8$ and other vibrational states. Moreover three parallel-transition type subbands are observed and their analysis is presented as well.

1. Introduction

Propyne, also known as methylacetylene, is an alkyne with the chemical formula CH_3—C≡CH. It is one of the simplest organic molecules and in the past few decades it has been topic of many spectroscopic studies. It has been identified in the interstellar medium [1] and in the atmosphere of Titan [2,3] and is also an important constituent of fuels. As a small terminal acetylene comprising two different types of C—H bonds (acetylenic and aliphatic), the investigation of vibration–rotation spectra of propyne has been of fundamental interest in understanding intramolecular vibrational redistribution (IVR) dynamics of hydrocarbons [4–11]. Extensive studies on the high-resolution spectra of propyne in its electronic ground state have been performed in the microwave (MW) [12,13], infrared (IR) and optical regions [10,14,15], using various spectroscopic detection techniques, such as multi-pass laser absorption spectroscopy [4,5], Fourier transform spectroscopy (FTS) [10,15], intracavity laser absorption spectroscopy (ICLAS) [10], cavity ringdown spectroscopy (CRDS) [10], IR double resonance spectroscopy [6,7], photo-acoustic spectroscopy [16] and two-color IR–vacuum ultraviolet laser photoion-photoelectron spectroscopy [17]. In Ref. [15], all vibrational energy patterns and ro-vibrational bands of propyne reported till 2001 have been summarized. In recent years, the spectroscopic parameters of several vibrational levels of propyne were further refined [18–20], and a few new bands have been reported in the second ($3\nu_1$) and third ($4\nu_1$) C—H acetylenic stretch overtone regions [16].

To our knowledge, the spectroscopic identification of the $\nu_3 + \nu_8$ combination band of propyne has not been reported before. Based on the previously published fundamental vibrational frequencies for the ν_3 (C≡C stretch) and ν_8 (CH_3 rock) modes, the $\nu_3 + \nu_8$ combination vibrational level of propyne is expected in the 3175 cm^{-1} region. The non-detection of this band in the previous FTS experiment [15] is consistent with a small infrared transition strength. In this contribution, we present for the first time the high resolution IR spectrum of the $\nu_3 + \nu_8$ combination band of supersonically jet-cooled propyne. This weak band is recorded by highly sensitive continuous-wave cavity ring-down spectroscopy (cw-CRDS), in combination with a supersonic free jet. The high pressure jet expansion allows us to generate a high density of propyne molecules in a collision-free environment, and the effective jet-cooling further increases the population density of the low-lying rotational levels. A detailed rotational analysis of the experimental spectrum is presented.

2. Experimental

The experimental setup has been described in detail in Ref. [21] and has recently been used to study the 3 μm IR spectrum of diacetylene in a pulsed plasma jet [22]. In brief, a premixed gas mixture (propyne:argon:helium ~ 1:100:100) with a pressure of ~5 bar is supersonically expanded into a vacuum chamber that is evacuated by a roots blower pump station with a total capacity of 4800 m^3/h. A home-made multi-layer slit (30 × 0.3 mm) nozzle in combination with a pulsed valve (General valve, serial 9) is used to generate a planar gas jet with pulse duration of ~800 μs. Different from the previous diacetylene experiment [22], no plasma is needed as propyne is available as a stable precursor species and consequently, the

* Corresponding author. Tel.: +31 71 5278475; fax: +31 71 5275819.
E-mail address: zhao@strw.leidenuniv.nl (D. Zhao).

http://dx.doi.org/10.1016/j.cplett.2014.02.016
0009-2614/

molecular purity in the jet is very high: only van der Waals complex formation cannot be fully ruled out. Cw-CRDS is used to record the weak $\nu_3 + \nu_8$ band of propyne in the supersonic jet, ~5 mm downstream of the slit nozzle throat. The density of the propyne molecules in the detection region of the jet beam is estimated to be of the order of 10^{16} cm^{-3}. A single-mode cw optical parametric oscillator (cw-OPO, Aculight, Argos 2400-SF-B), operating at ~3.15 μm with an output power ~1 W and a bandwidth <1 MHz, is employed as tunable infrared light source for the cw-CRDS measurement. A hardware (boxcar integrator) based multi-trigger and timing scheme as described in Ref. [21] is used to apply cw-CRDS to a pulsed gas jet. The ring-down cavity is 56 cm long and comprises two plano-concave mirrors with a reflectivity of ~99.98%. Typical ring-down times are ~7–9 μs. In the present experiment, the length of the ring-down cavity is modulated at 50 Hz, allowing us to tune the infrared laser wavelength during the spectrum recording two times faster than in our initial configuration [21,22]. This further improves the spectroscopic potential of this setup.

The absolute laser frequency is simultaneously calibrated using a wavelength meter (Bristol Instruments, 621A-IR) and is independently checked by the recorded absorption lines of trace H_2O molecules in the vacuum chamber. The Doppler width in the recorded 3.15 μm spectrum of propyne is reduced to ~110 MHz. The absolute frequency accuracy of the recorded propyne transitions is better than 60 MHz.

3. Results and discussion

In this study, the $\nu_3 + \nu_8$ combination band has been searched for in the 3150–3200 cm^{-1} region. The resulting experimental spectrum is shown in the upper panel of Figure 1a, where a perpendicular band with a series of subbands clearly can be seen. The strongest Q-branch is at ~3176.8 cm^{-1}, very close to the expected position. Therefore, it is very likely that this perpendicular band system is due to the $\nu_3 + \nu_8$ combination band of propyne, specifically as the perpendicular character of this band is consistent with the E state symmetry of the $\nu_3 + \nu_8$ combination vibrational level. Further proof comes from the rotational analysis.

The slit jet expansion realizes an effective adiabatic cooling of the J rotational state populations which simplifies the experimental spectrum – increasing state densities and decreasing spectral overlaps. All bands comprise fully resolved P-, Q- and R-branches and the $P(J)$, $Q(J)$ and $R(J)$ rotational assignments are rather straight forward. The lower-state combination differences, $R(J)$–$P(J+2)$, are in good agreement with the calculated values using the precise ground-state constants of propyne available from Ref. [19]. This is a further confirmation of the correct assignment of this band to propyne and rules out interfering features of propyne-rare gas complexes or propyne clusters. The $K^{(l)}$ assignments can be directly derived from the starting values of the observed J'' and J' in each perpendicular subband and are shown as separate spectra in Figure 1b.

In addition to the perpendicular-transition type subbands that can be assigned to $\nu_3 + \nu_8$, three parallel-transition type subbands, at ~3173.6, 3159.7, and 3188.3 cm^{-1} with $K = 0$, 1, and 1, respectively, show up in our experimental spectrum. They are labeled as unidentified subbands in Figure 1c. Their lower-state combination differences confirm that the corresponding transitions originate from energy levels in the vibrational ground state of propyne.

The experimental spectrum is analyzed using the PGOPHER software [23]. The rotational energy levels in the vibrational ground state (A_1 symmetry) of propyne are calculated using the molecular parameters constrained by Pracna et al. in Ref. [19]. The rotational energy levels in the upper degenerate vibrational state (E symmetry) are calculated by the standard relation for a prolate C_{3v} symmetric top molecule:

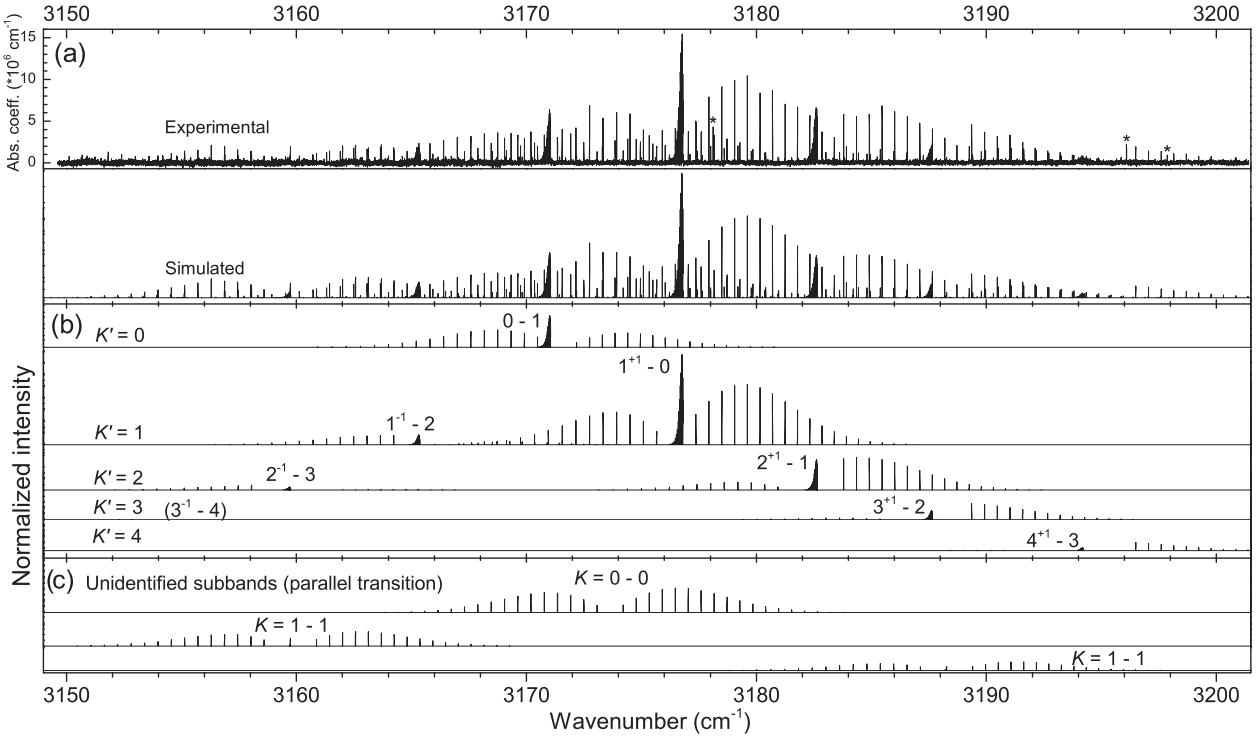

Figure 1. (a) The experimental (upper trace) and simulated sum spectra (lower trace) in the 3175 cm^{-1} region; (b) the individual K-subband spectra and corresponding $K^{(l)}$ assignments of $\nu_3 + \nu_8$; (c) the individual spectra of the three unidentified parallel-transition type subbands. The absorption features marked by asterisks in panel (a) are due to trace water in the vacuum chamber. An estimated rotational temperature of ~22 K is used in the simulated spectrum. The 3^{-1}–4 subband is below the detection limit and is not observed in the experimental spectrum.

$$E(v_i, J, K, l) = E(v_i) + 2A\zeta \cdot lK + (A - B)K^2 + BJ(J+1) - D_J J^2(J+1)^2 - D_{JK}J(J+1)K^2 - D_K K^4 \quad (1)$$

where A and B are the rotational constants, D_J, D_{JK}, and D_K the centrifugal distortion constants, and ζ the Coriolis coupling constant.

The rotational analysis starts from a least squares fit only including subbands with $K' = 0$ and 1 which results in a set of reasonable spectroscopic parameters. However, this set of parameters does not fully reproduce the observed transition frequencies of subbands with ΔK (or l) = +1. A plot of the obs.–calc. values for the upper-state rotational levels is shown in Figure 2. The J-dependent splitting of the upper $K' = l = +1$ levels in Figure 2 is due to the l-type doubling effect, which has been discussed by Cartwright and Mills in Ref. [24]. For a C_{3v} symmetric top molecule, this effect can be described by:

$$\pm(q_t/2) \cdot J(J+1) \quad (2)$$

where q_t is the l-doubling constant, and the '+' and '–' signs correspond to rotational levels with A_1 and A_2 symmetries, respectively.

Figure 2 also indicates an anomalous K-subband ordering. Particularly for the $K' = 3$ and 4 levels, overall shifts up to ~ -0.85 and $-0.25\ \mathrm{cm}^{-1}$, respectively, show up. Such anomalous K-subband ordering is usually caused by perturbations of states with non-zero vibrational angular momentum, in which first-order Coriolis splittings lead to large K-dependent shifts in the relative spacings of different vibrational states [5,25]. Apparently, the three parallel-transition type subbands (with $K' = 0$ and 1) observed in our spectrum do not provide information about the severe perturbations at $K' = 3$ and 4. Moreover, although the perturbations at $K' = 3$ are relatively heavy, no other weak absorption features that can be assigned to a resonant perturber state are found. Considering that the vibrational state density of propyne in the 3000–3300 cm^{-1} region, including all vibrational angular momentum components arising from degenerate modes, is $\sim$1 states/cm^{-1} [4], near-resonant or non-resonant perturbations are likely involved here, as has been concluded for the case of the $2\nu_1$ overtone band [5].

Because weak features representative for near-resonant vibrational interactions are not observed due to the limited signal-to-noise in our experiment, the effective spectroscopic parameters that can be used to accurately calculate the observed ro-vibrational transitions are derived as follows:

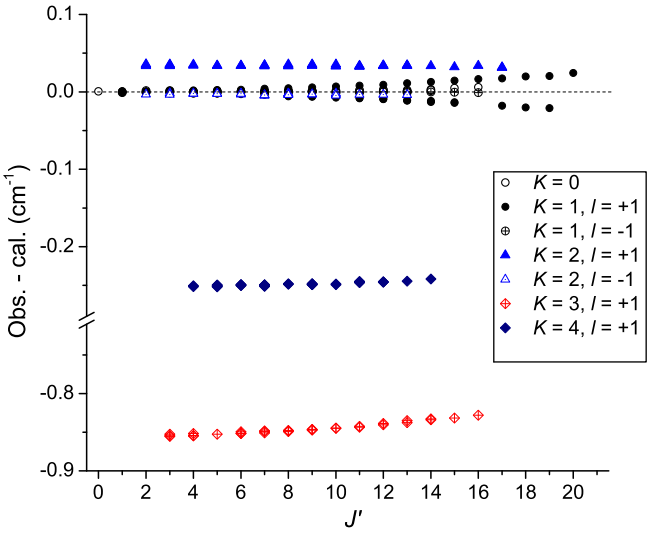

Figure 2. The obs.–calc. values for the rotational levels in the upper $\nu_3 + \nu_8$ state from the fit using Eq. (1) and only including the subbands with $K' = 0$ and 1.

(i) The subbands or subband pairs with the same K' values are fitted separately, with exclusion of the centrifugal distortion constants D_K and D_{JK} in Eq. (1).
(ii) For the $K' \neq 0$ subbands, the value of the state origin $E(\nu_3 + \nu_8)$ is fixed to the value derived from the $K' = 0$ data.
(iii) Since the 3^{-1}–2 and 4^{-1}–3 subbands are below our detection limit and are not observed in the present experiment, the $K' = 3$ and 4 data are fitted with the rotational constants A fixed to values derived from the $K' = 2$ data.

The resulting effective spectroscopic parameters, as well as the parameters for the ν_3 and ν_8 fundamental vibrational levels reported in Refs. [14,19], are summarized in Table 1. The *rms* of the fit is $\sim 8 * 10^{-4}\ \mathrm{cm}^{-1}$. The obs.–calc. values of all determined ro-vibrational transitions are listed in the Supplementary material. In a similar way, the three parallel-transition type subbands are fitted separately, and the resulting spectroscopic parameters are summarized in Table 2.

In the lower trace of Figure 1a the sum spectrum of all individually simulated subbands (Figure 1b and c) is shown for a comparison, using the spectroscopic parameters listed in Table 1 and Table 2. Figure 3 shows the zoomed-in experimental and simulated spectra in the Q-branch regions of the 1^{+1}–0 and 0–1 subbands and illustrates the excellent agreement. A Gaussian linewidth of 110 MHz ($\sim$0.0037 cm^{-1}) and an estimated rotational temperature $\sim$22 K are used in these spectral simulations.

In a previous slit-jet experiment of propyne [4], it was found that the K' state cooling is limited by the nuclear spin symmetry properties in their slit jet. However, in the simulation of our experimental spectrum, we noticed that only one rotational temperature of $\sim 22 \pm 2$ K for both J' and K' rotational state populations is required to reproduce the overall intensity pattern, and the inclusion of the statistical weights due to nuclear spin symmetry is not needed. The effective relaxation of nuclear spins in our experiment may be due to a much larger slit width than used in Ref. [4] or the presence of argon in the gas mixture, which may yield longer-range and more low-velocity collisions to relax the nuclear spin.

Using the derived rotational constants B for the $K' = 0$ and 1 rotational levels in the $\nu_3 + \nu_8$ combination as listed in Table 1, we can derive $\alpha^B_{3+8} = 1.621\ (6) * 10^{-3}\ \mathrm{cm}^{-1}$. This value is very close to the approximate value of $(\alpha^B_3 + \alpha^B_8 \approx)\ 1.70 * 10^{-3}\ \mathrm{cm}^{-1}$. The $\zeta_{3+8} \sim 0.406$ for $K' = 1$ and 2 levels is also very close to $\zeta_8 \sim 0.411$, consistent with the discussion in Ref. [15] that the resulting ζ value of a combination state is close to the value of the fundamental level responsible for the degenerate character.

It should be noted that, in this Letter, the rotational levels with different K' values are analyzed separately. In this case, it can be found from Eq. (1) that the three parameters, $E(\nu_3 + \nu_8)$, A, and $A\zeta$ are correlated, i.e., they cannot be determined from one fit independently. The effective values of A and $A\zeta$ in Table 1 are derived under the assumption that the $K' = 0$ levels are not perturbed. However, with the present set of experimental data, we cannot fully exclude that perturbations, particularly Fermi-resonance type perturbations are involved at $K' = 0$. Actually, the derived $D_J \sim 0.31\ (23) * 10^{-7}\ \mathrm{cm}^{-1}$ value is significantly smaller than that of the ν_3 and ν_8 fundamental vibrational levels and may hint for perturbed high-J' $K' = 0$ rotational levels. Consequently, the effective parameters of $E(\nu_3 + \nu_8)$ and A may not be accurate enough to evaluate the anharmonic constant x_{3+8} and the vibration–rotation interaction constant α^A_{3+8}.

As has been shown before, the perpendicular bands can be assigned relatively straight forward. However, because of the vibrational state congestion in this energy region, the vibrational assignment of the three parallel-transition type subbands is challenging. Two of them, at $\sim$3173.6 cm^{-1} with $K' = 0$ and at $\sim$3159.7 cm^{-1} with $K' = 1$, have very similar rotational constants

Table 1
Spectroscopic parameters (cm^{-1}) of the vibrational levels v_3, v_8, and $v_3 + v_8$.[a] For the ground state the precise values available from Ref. [19] have been used.

Parameters	v_3 [14][b]	v_8 [19][b]	$v_3 + v_8$				
			$K = 0$	$K = 1$	$K = 2$	$K = 3$	$K = 4$
E(v)	2137.87 (12)	1036.14754 (2)	3176.0774 (2)	3176.0774[c]	3176.0774[c]	3176.0774[c]	3176.0774[c]
A	5.3017 (2)	5.335651 (4)	–	5.34207 (17)	5.34604 (4)	5.34604[c]	5.34604[c]
B	0.283550 (2)	0.2848679 (14)	0.283442 (6)	0.283442 (3)	0.283439 (4)	0.283540 (7)	0.283470 (4)
$D_J \times 10^7$	0.975 (5)	0.99000 (11)	0.31 (23)	1.01 (8)	1.18 (14)	0.83 (28)	0.83[c]
A_ζ	–	2.191788 (4)	–	2.16480 (8)	2.16016 (3)	2.31316 (5)	2.20415 (3)
$q_t \times 10^4$	–	−1.4566 (20)	–	−1.177 (14)			

[a] Numbers in parentheses are one standard deviation in units of the last significant digit. For the band origins E(v), the absolute wavenumbers are determined with a precision better than 0.002 cm^{-1} in the present study.
[b] Other parameters of the two fundamental vibrational states are not listed (see Refs. [14,19] for the complete set of spectroscopic parameters).
[c] Fixed values.

Table 2
Spectroscopic parameters (cm^{-1}) of the unidentified parallel-transition type subbands.[a].

Parameters	$K = 0$	$K = 1$	$K = 1$
E(v)	3173.6411 (3)	3159.7361 (3)	3188.2731 (3)
B	0.284428 (8)	0.284422 (6)	0.283324 (10)
A	–	5.308313[b]	5.308313[b]
$D_J \times 10^7$	−8.39 (33)	−1.91 (26)	−12.66 (62)

[a] Numbers in parentheses are one standard deviation in units of the last significant digit. For the band origins E(v), wavenumbers are determined with a precision better than 0.002 cm^{-1}.
[b] Fixed to the value of A_0 from Ref. [19].

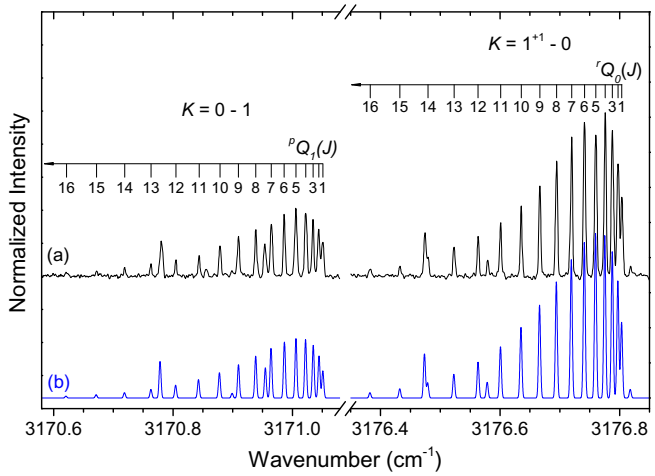

Figure 3. Zoomed-in experimental (a) and simulated (b) spectra in the Q-branch regions of the 1^{+1}–0 and 0–1 subbands. An estimated rotational temperature of ~22 K and a Gaussian linewidth of ~110 MHz (~0.0037 cm^{-1}) are used in the simulated spectrum.

B. However, if the two subbands are due to the same upper vibrational state, the $K' = 1$ level would be ~8.6 cm^{-1} below the $K' = 0$ levels in the upper state. This is in general not possible for a non-degenerate vibrational state, unless a very heavy perturbation occurs which reverses the order of the $K' = 0$ and $K' = 1$ level energies.

4. Conclusion

We have presented the first fully resolved experimental spectrum and a detailed rotational analysis of the $v_3 + v_8$ combination band of propyne (CH_3—C≡CH). This has become possible using a highly sensitive infrared spectrometer in combination with a free slit jet expansion. Our analysis indicates that near-resonant or non-resonant perturbations are likely involved in this weak band. For a comprehensive understanding in the complex vibrational couplings of $v_3 + v_8$ to other states, more sensitive measurements are required to observe even weaker features which may be representative for near-resonant bath states in this region.

Acknowledgements

This Letter is financially supported by a NWO-VICI Grant, NOVA, SRON and has been performed within the context of the Dutch Astrochemistry Network.

Appendix A. Supplementary data

Supplementary data associated with this article can be found, in the online version, at http://dx.doi.org/10.1016/j.cplett.2014.02.016.

References

[1] D. Buhl, L.E. Snyder, in: M.A. Gordon, L.E. Snyder (Eds.), Molecules in the Galactic Environment, Wiley-Interscience, New York, 1973, p. 187.
[2] R. Hanel, B. Conrath, F.M. Flasar, V. Kunde, W. Maguire, J. Pearl, J. Pirraglia, R. Samuelson, L. Heralth, M. Allison, D. Cruikshank, D. Gautier, P. Gierasch, L. Horn, R. Koppany, C. Ponnamperuma, Science 212 (1981) 192.
[3] A. Coustenis, Th. Encrenaz, B. Bézard, G. Bjoraker, G. Graner, M. Dang-Nhu, E. Arié, Icarus 102 (1993) 240.
[4] A. McIlroy, D.J. Nesbitt, J. Chem. Phys. 91 (1989) 104.
[5] A. McIlroy, D.J. Nesbitt, E.R.T. Kerstel, B.H. Pate, K.K. Lehmann, G. Scoles, J. Chem. Phys. 100 (1994) 2596.
[6] J. Go, J. Chem. Phys. 97 (1992) 6994.
[7] J. Go, T.J. Cronin, D.S. Perry, Chem. Phys. 175 (1993) 127.
[8] J.E. Gambogi, E.R.T. Kerstel, K.K. Lehmann, G. Scoles, J. Chem. Phys. 100 (1994) 2612.
[9] E.R.T. Kerstel, K.K. Lehmann, B.H. Pate, G. Scoles, J. Chem. Phys. 100 (1994) 2588.
[10] A. Campargue, L. Biennier, A. Garnache, A. Kachanov, D. Romanini, M. Herman, J. Chem. Phys. 111 (1999) 7888.
[11] A. Portnov, L. Blockstein, I. Bar, J. Chem. Phys. 124 (2006) 164301.
[12] H.S.P. Müller, S. Thorwirth, L. Bizzocchi, G. Winnewisser, Z. Naturforsch. 55a (2000) 491.
[13] H.S.P. Müller, P. Pracna, V.M. Horneman, J. Mol. Spectrosc. 216 (2002) 397.
[14] N.F. Henfrey, B.A. Thrush, J. Mol. Spectrosc. 121 (1987) 150.
[15] M.I. El Idrissi, J. Liévin, M. Herman, A. Campargue, G. Graner, Chem. Phys. 265 (2001) 273.
[16] Y. Ganot, S. Rosenwaks, I. Bar, J. Chem. Phys. 122 (2005) 244318.
[17] M. Thompson, J.G. Baker, T.D. Bevis, Mol. Phys. 101 (2003) 381.
[18] X. Xing, B. Reed, K.C. Lau, S.J. Baek, M.K. Bahng, C.Y. Ng, J. Chem. Phys. 127 (2007) 044313.
[19] P. Pracna, H.S.P. Müller, Š. Urban, V.M. Horneman, S. Klee, J. Mol. Spectrosc. 256 (2009) 152.
[20] M. Villa, L. Fusina, G. Nivellini, K. Didriche, X. Vaernewijck, M. Herman, Chem. Phys. 402 (2012) 14.
[21] D. Zhao, J. Guss, A.J. Walsh, H. Linnartz, Chem. Phys. Lett. 565 (2013) 132.
[22] D. Zhao, K.D. Doney, H. Linnartz, J. Mol. Spectrosc. 296 (2014) 1.
[23] PGOPHER, a Program for Simulating Rotational Structure, C.M. Western, University of Bristol, <http://pgopher.chm.bris.ac.uk>.
[24] G.J. Cartwright, I.M. Mills, J. Mol. Spectrosc. 34 (1970) 415.
[25] B.H. Pate, K.K. Lehmann, G. Scoles, J. Chem. Phys. 95 (1991) 3891.